IEEE Access
Multidisciplinary ⋮ Rapid Review ⋮ Open Access Journal

Received July 8, 2021, accepted August 4, 2021, date of publication August 18, 2021, date of current version August 26, 2021.

Digital Object Identifier 10.1109/ACCESS.2021.3105649

Multi-Objective Finite-Time Control for the Interlinking Converter on Hybrid AC/DC Microgrids

MANUEL MARTINEZ-GOMEZ[1,2], (Graduate Student Member, IEEE),
ALEX NAVAS[1,2], (Graduate Student Member, IEEE),
MARCOS E. ORCHARD[1], (Member, IEEE),
SERHIY BOZHKO[2], (Senior Member, IEEE),
CLAUDIO BURGOS-MELLADO[3], (Member, IEEE),
AND ROBERTO CÁRDENAS[1], (Senior Member, IEEE)

[1]Department of Electrical Engineering, University of Chile, Santiago 8370451, Chile
[2]PEMC Group, University of Nottingham, Nottingham NG7 2RD, U.K.
[3]Institute of Engineering Sciences, Universidad de O'Higgins, Rancagua 2820000, Chile

Corresponding author: Manuel Martinez-Gomez (manuel.martinez.gmz@ieee.org)

This work was supported by the National Agency for Research and Development (ANID), Chile, in part by ANID-FONDECYT under Grant 1170683, in part by ANID-Basal Project under Grant FB0008 (Advanced Center for Electrical and Electronic Engineering, AC3E), and in part by ANID-FONDEQUIP under Grant EQM160122 (for funding the experimental prototype to validate this research). The work of Manuel Martinez-Gomez was supported by ANID-Becas/Doctorado Nacional under Grant 2019-21191757. The work of Alex Navas was supported in part by ANID-Becas/Doctorado Nacional under Grant 2019-21190961, and in part by the Secretaría de Educación Superior, Ciencia, Tecnología e Innovación de Ecuador, under Grant SENESCYT/ARSEQ-BEC-005848-2018.

ABSTRACT Hybrid AC/DC microgrids are of special interest for energization due to their flexibility, low infrastructure investments, reduced conversion losses, and reliability against failures on the utility grid. In these systems, global economic dispatch needs communication between the AC and DC subgrids to achieve a near-optimal solution since the incremental costs of all generators need to be equalized. Hence, this paper proposes a distributed coordination between generators by means of a finite-time controller for the microgrid's interlinking converter, which ensures an economic operation while taking care of the microgrid power utilization. The latter implies that a multi-objective control is performed by the interlinking converter, which uses shared variables of incremental costs and average powers from distributed generators in AC and DC sides. Also, an adaptive weighting method is proposed to adjust the control effort regarding the average power utilization of a side microgrid. The controller's performance is verified through simulations and experimental setups. Results show that the proposed strategy is able to perform a trade-off between the two control objectives while achieving a finite-time convergence even though communication delays exist.

INDEX TERMS Economic dispatch, distributed control, finite-time control, hybrid AC/DC microgrid, multi-objective control.

I. INTRODUCTION

Traditional centralized electrical systems are integrating new clusters of generation and loads, in which Distributed Generators (DGs) are located near the consumption. The latter gives rise to the proliferation of Microgrids (MGs), which are autonomous and can operate either connected or disconnected from the utility grid [1]. A promising type of MG is the hybrid AC/DC MG, see Fig. 1, which is able to combine the advantages of both AC and DC MGs while reducing the overall costs by re-utilizing most of the existing AC infrastructure. The additional DC-side network is used to interface DC-based DGs with Energy Storage Systems (ESSs), reducing energy conversion steps in the process [2], [3]. The operation of a hybrid MG is possible due to the Interlinking Converter (ILC), which allows

The associate editor coordinating the review of this manuscript and approving it for publication was Bin Zhou.

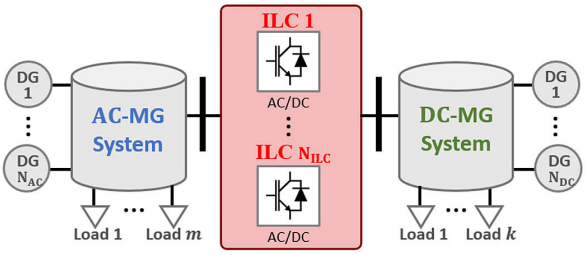

FIGURE 1. Generic hybrid AC/DC MG representation.

bidirectional energy transfer between AC and DC sides; moreover, some authors have suggested the utilization of clusters of ILCs to manage the energy transfer [4]–[6], as depicted on Fig. 1.

Conventionally, the control of MGs adopts a hierarchical structure of three levels [1], [7], [8], where the primary control usually realizes a power-sharing by deviating the converters' control variables. The secondary control is in charge of the voltage and frequency restorations (maintaining the power-sharing), whereas the tertiary control adjusts the power flow of the MG to achieve specific goals such as the economic dispatch (some authors perform the economic dispatch at the secondary control level [1], [9], [10]). In terms of multi-objective control, most research efforts have been mainly focused on developing optimization-based techniques in MGs [11]; although one can find distributed algorithms synchronizing voltage and reactive power simultaneously according to a fixed trade-off parameter [6], [8].

Despite the advancements on the control area, the economic dispatch control in hybrid AC/DC MGs has not been fully solved and there still exist research gaps that need to be explored to ensure the system's reliable and proper operation.

A. PROBLEM STATEMENT

For the control of the hybrid AC/DC MG, the problem to be solved consists of simultaneously ensuring an economic power-sharing and a reliable operation for all the DGs. For the economic dispatch coordination, both subgrids (AC and DC) need to agree on the most cost-effective use of DGs. This is done by means of the equal incremental cost (IC) principle [12]. However, this is not an easy task because the optimal power distribution is not only economical; it also needs to avoid the saturation of DGs, and consequently, of MGs. The saturations originate because, occasionally, the IC variables suffer variations, and the difference between the ICs of the AC and DC MGs is significant. Common reasons for such variations of ICs are the disconnection of DGs, the power-sharing of ESSs based on the State of Charge (SoC) [7], and the market price for energy in grid-connected operations [13].

B. MOTIVATION

In terms of the ILC's control, the sole regulation of ICs in situations where significant differences exist between the subgrids may lead the ILC to leave an MG without energy reserves, which are critical for dealing with generation-demand balancing, especially during transient states. Thus, if a saturated subgrid increases its load, it will need to obtain power from the other subgrid through the ILC, which is a slow process that might deteriorate the transient dynamics. To the best to the author's knowledge, this problem has not been addressed in hybrid MG control, with the exception of [14], where an attempt to avoid MG's saturation is indirectly introduced by means of a safety operation limit of 0.95 imposed in the power boundaries of the ILC's operation mode. Nonetheless, this method constantly reduces the power capacity of the ILC; also, it requires a fixed topology, so it is not effective in the plug & play operation of DGs.

C. LITERATURE REVIEW

First attempts in the control of ILCs mainly focus on decentralized algorithms [3], [15], [16], where normalized droop curves guide the power to be transferred by the ILC. With decentralized control, global coordination of power or IC can be achieved using only local measurements at the ILC. However, these approaches require some knowledge of the hybrid MG, e.g. specific topologies such as single bus, or that all DGs in the same MG have known droop characteristics. Regarding the economic dispatch, the literature shows decentralized approaches for the ILC based on cost curves. The works [12], [17], [18] inherit some mentioned disadvantages related to decentralized power-sharing. Additionally, these approaches cannot include a secondary control, i.e. frequency and voltage restoration, since the droop deviations are key components for the ILC measurements. Some works such as [14], [19] include centralized control to carry out the tertiary control (economic dispatch) in the hybrid MG. Nonetheless, it is worth noting that centralized controllers are susceptible to single-point-failure, reducing the system's reliability [1].

As an alternative to the previous control schemes, researchers have studied distributed control strategies for hybrid MGs [20]–[23]. References [20], [21] have successfully applied distributed protocols into the ILC's control for balancing the normalized power between AC and DC MGs. However, economic dispatch was not considered by them. In [22], a distributed secondary control for the economic dispatch is developed by means of auxiliary variables based on DGs compensations; however, the implementation is strongly dependent on cost-based droop curves and requires modification of local controllers. In [23], a unified distributed IC strategy for hybrid MGs is proposed, where IC variables are part of a distributed secondary control and shared with the ILC. However, the ILC's communication scheme, stability, and parameters design are not provided. Furthermore, none of the previous works provides details about the fulfillment of power constraints in the hybrid MG, which is a major concern for an optimal power system operation [1], [11].

Overall, available distributed control schemes are still unattractive given the limited functionality that they bring to the operation of the ILC at the cost of investing in

communication lines. Also, there is a need for additional compensations in the ILC controller to avoid over-stress saturation of the subgrids.

D. CONTRIBUTIONS

Motivated by the above discussion, and based on a previous work [24], the authors of this paper propose a control scheme for the ILC that seeks for the global economic dispatch in hybrid AC/DC MGs. Moreover, the proposed protocol implements a trade-off between IC balancing (the cheapest operation) and energy reserves storing (the safest transient operation). The implementation involves a distributed average power observer and a consensus with dynamic weights. Additionally, this work proposes the incorporation of finite-time protocols, such as those used in [25] and [26], to assist with decoupling between the control goals of the ILC, to deal with small disturbances, and to accelerate the convergence of communication protocols. The contributions of this work can be summarized as follows:

- A finite-time communication-based control for the ILC is proposed, which guarantees the economic dispatch of a hybrid AC/DC MG. A Lyapunov candidate is then derived, which models the hybrid MG as a graph of error signals and demonstrates the system's convergence.
- A multi-objective formulation for the ILC is proposed. An average power term is added to the ILC's controller to manage the saturation of MGs. A proof of convergence is also developed, showing that the system can simultaneously reach equilibrium in IC and average power, provided a trade-off weighting gain.
- Experimental and simulation validations of the proposed multi-objective finite-time controller for the ILC are realized. They show the behavior of the ILC's controller under different conditions.

The rest of the paper is organized as follows. In Section II, the preliminaries of graph theory, finite-time control and economic dispatch are presented. In Section III, the design of a distributed control for the ILC is presented along with a Lyapunov convergence analysis. Section IV, explains the design and proof of convergence of a multi-objective distributed control. In Section V, case studies are described with the system and control parameters. In Section VI, the results are presented and discussed, followed by the conclusions in Section VIII.

II. PRELIMINARIES

In this section, some useful preliminaries required for the controller designs of Section III and Section IV are provided.

A. GRAPH THEORY

The communication topology between DGs in a MG can be represented by a multi-agent system through a graph [27]. The graph can be expressed as $\mathcal{G}(A) := (\mathcal{N}, E, A)$, where $\mathcal{N} = \{n_1, n_2, \ldots, n_N \,/\, N = |\mathcal{N}|\}$ represents the nodes (or DGs), $E = \{(n_i, n_j) \,/\, E \in \mathcal{N}^2\}$ denotes the communications links and $A = [a_{ij}]_{N\times N}$ is the adjacency matrix whose elements $a_{ij} \forall\, i, j \subseteq \mathcal{N}$ stand for connectivity weights. Also, $a_{ij} \geq 0 \Leftrightarrow (n_i, n_j) \in E$, which implies that nodes i and j can communicate each other; otherwise, $a_{ij} = 0$. The set of neighbors of the i-th node is given by $\mathcal{N}(i) = \{n_j \,/\, (n_i, n_j) \in E\}$ where j is the index of a communicated DG. For simplicity, $\mathcal{N}$ and $\mathcal{N}(i)$ are ordered sets inside a MG, also $N_i = |\mathcal{N}(i)|$.

It is defined $L = D - A$ as the graph Laplacian matrix with $D = \text{diag}\{d_1, d_2, \ldots, d_N\} \in \mathbb{R}^{N\times N}$ as the in-degree matrix and $d_i = \sum_{j=1}^{N} a_{ij}$ the weighted in-degree of node i. The graph $\mathcal{G}(A)$ is called balanced if its Laplacian matrix L meets $1_N^T L = 0$, i.e. a bidirectional information flow between DGs. A graph is said to have a spanning tree if there exists a directed path from one node to any other in the graph [28].

B. FINITE-TIME PROTOCOL

For a multi-agent system with the dynamics $\dot{x}_i = u_i$, with x_i the state of agent i, it is defined the state feedback u_i as:

$$u_i = -c \sum_{j=1}^{N_i} a_{ij} \,\text{sign}\left(x_j - x_i\right) \left|x_j - x_i\right|^{\alpha}. \tag{1}$$

For convenience, it is denoted $\text{sig}[\,\cdot\,]^{\alpha} = \text{sign}(\cdot)|\,\cdot\,|^{\alpha}$. Provided $c > 0$ and $\alpha \in (0, 1)$, $\forall i \in \mathcal{N}(i)$, the protocol (1) achieves $(x_j - x_i) = 0$ in a finite-time T given by:

$$T \leq \frac{V\,(x_0)^{1-\alpha}}{c\,(1-\alpha)},$$

where $V(x_0)$ is a Lyapunov-Krasovskii candidate function [29]. The protocol (1) accelerates the convergence compared with asymptotic protocols while incorporates a level of disturbance rejection [30], [31].

C. ECONOMIC DISPATCH IN HYBRID AC/DC MG

The economic dispatch for hybrid MGs can be formulated as an optimization problem of the form

$$\begin{aligned} \min &\left\{\sum_{i=1}^{N_{\text{HYB}}} C_i(P_i)\right\} \\ \text{subject to, } & C_i(P_i) = a_{ci}P_i^2 + b_{ci}P_i + c_{ci} \\ & P_i^{\min} \leq P_i \leq P_i^{\max} \\ & P_{\text{D}}^{\text{AC}} + P_{\text{D}}^{\text{DC}} - \sum_{j\in\mathcal{N}_{\text{HYB}}} P_j = 0, \end{aligned} \tag{2}$$

where $C_i(P_i)$ is a quadratic cost function for the i-th generator with parameters a_{ci}, b_{ci} and c_{ci}. P_{D}^{AC} and P_{D}^{DC} are the demanded powers of the subgrids, and $\mathcal{N}_{\text{HYB}} = \{\mathcal{N}_{\text{AC}} \cup \mathcal{N}_{\text{DC}}\}$. Thus, the Lagrangian function is constructed as

$$\begin{aligned} \mathbb{L}\left(P_i, \sigma_i^+, \sigma_i^-, \lambda\right) = &\sum_{i=1}^{N_{\text{HYB}}} C_i(P_i) + \sum_{i=1}^{N_{\text{HYB}}} \sigma_i^+(P_i - P_i^{\max}) \\ &+ \sum_{i=1}^{N_{\text{HYB}}} \sigma_i^-(P_i^{\min} - P_i) + \lambda\left(P_{\text{D}}^{\text{AC}} + P_{\text{D}}^{\text{DC}} - \sum_{i=1}^{N_{\text{HYB}}} P_i\right). \end{aligned} \tag{3}$$

From stationary condition, one has

$$\frac{\partial}{\partial P_i}\mathbb{L}\left(P_i, \sigma_i^+, \sigma_i^-, \lambda\right) = 0 \Leftrightarrow \lambda = \frac{\partial C_i\left(P_i\right)}{\partial P_i} + \sigma_i^+ - \sigma_i^-, \tag{4}$$

where all the DGs must have the same IC (λ) to accomplish the global economic dispatch (other optimality conditions can be proved as in [10]).

Provided that each MG implements its own economic dispatch optimization, a distributed control based on the works [9], [10] can be assumed on each side. As a result, the ICs are obtained as:

$$\begin{aligned}\lambda_i^{\mathrm{AC}} &= 2a_{ci}P_i + b_{ci} + \sigma_i^+ - \sigma_i^-,\\ \lambda_j^{\mathrm{DC}} &= 2a_{cj}P_j + b_{cj} + \sigma_j^+ - \sigma_j^-,\end{aligned} \tag{5}$$

where the condition $\lambda_i^{\mathrm{AC}} = \lambda_j^{\mathrm{DC}}\ \forall\ i \in \mathcal{N}_{\mathrm{AC}} \wedge j \in \mathcal{N}_{\mathrm{DC}}$ must be held for the global economic dispatch. Therefore, the goal of the ILC is to equalize the ICs of (5). From this point, a distributed control strategy is designed for this purpose.

III. DESIGN OF DISTRIBUTED CONTROL FOR THE INTERLINKING CONVERTER

The power reference for the internal control loops of the ILC can be calculated by directly comparing the ICs of (5). Hence, concerning reliability and accuracy, it is proposed a distributed scheme where the DGs send their IC measurements to the ILC. Because the control actions taken by the ILC affect the IC dynamics of the AC and DC subgrids, the whole hybrid AC/DC MG can be viewed and analyzed as a multi-agent system with a graph $\mathcal{G}_{\mathrm{HYB}}$.

A. COMMUNICATION NETWORK

For simplicity, the communication between MGs is implemented only through the ILC, i.e. DGs of different subgrids cannot communicate directly. The proposed communication topology for the hybrid MG can be represented as a combination of graphs, such as $\mathcal{G}_{\mathrm{HYB}} := \mathcal{G}_{\mathrm{AC}} \cup \mathcal{G}_{\mathrm{DC}} \cup \mathcal{G}_{\mathrm{ILC}}$. Each subgrid's graph contains its communicated nodes (or DGs), and can be expressed as $\mathcal{G}(A^{\mathrm{AC}})$ or $\mathcal{G}(A^{\mathrm{DC}})$. Also, $\mathcal{G}_{\mathrm{ILC}} := (\mathcal{N}^*, E^{\mathrm{ILC}}, A^{\mathrm{ILC}})$ with $\mathcal{N}^* \subset (\mathcal{N}_{\mathrm{AC}} \cup \mathcal{N}_{\mathrm{DC}} \cup \mathcal{N}_{\mathrm{ILC}})$ represents the communication graph between the side MGs and the ILC(s). Fig. 2 summarizes the communication scheme considered by this work.

In this work, the communication scheme assumes only one ILC ($N_{\mathrm{ILC}} = 1$), but it can be extended to multiple ILCs. The former gives $\{A^{\mathrm{ILC}}\} = \{a^{\mathrm{ILC}}_{\mathrm{AC}\,i} \cup a^{\mathrm{ILC}}_{\mathrm{DC}\,j} \cup a^{\mathrm{ILC}}_{\mathrm{ILC}\,k}\ /\ i \in \mathcal{N}_{\mathrm{AC}} \wedge j \in \mathcal{N}_{\mathrm{DC}} \wedge k \in \mathcal{N}_{\mathrm{ILC}}\}$ where $a^{\mathrm{ILC}}_{\mathrm{AC}}$, $a^{\mathrm{ILC}}_{\mathrm{DC}}$ and $a^{\mathrm{ILC}}_{\mathrm{ILC}}$ are vectors that represent the communication between the ILC and the DGs in the AC and DC subgrids, and with the system's ILCs, respectively.

This communication topology allows the subgraphs $\mathcal{G}_{\mathrm{AC}}$ and $\mathcal{G}_{\mathrm{DC}}$ operate independently when the ILC ($\mathcal{G}_{\mathrm{ILC}}$) is disconnected, or when one side stops communicating to the ILC.

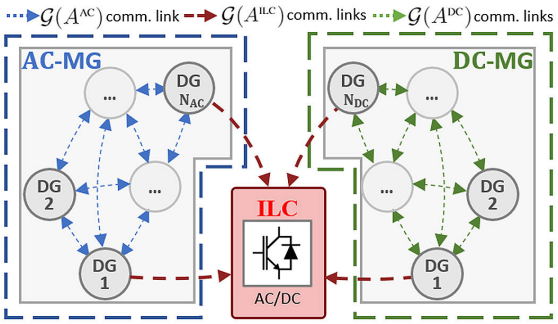

FIGURE 2. Cyber-physical system representing a hybrid AC/DC MG. The ILC is an agent that solely receives information, and it can indirectly (by a physical power transfer) connect the AC and DC graphs.

B. DISTRIBUTED CONTROL FOR ECONOMIC DISPATCH

Provided that each MG (AC or DC) can regulate and share its DG's IC, a PI controller for equalizing these ICs can be constructed for the ILC as

$$P^*_{\mathrm{ILC}} = k_p^P(u_{\mathrm{ILC}}) + k_i^P \int_0^t (u_{\mathrm{ILC}})d\tau, \tag{6}$$

where P^*_{ILC} is the power reference to be transferred between MGs, u_{ILC} is the input error of IC, k_p^P and k_i^P are control parameters. The reference P^*_{ILC} is then used by the internal control loops of the ILC (the control of the internal loops can be performed following the procedure described in [15] or [20]).

Given the communication matrix A^{ILC}, one can estimate the control input for the ILC controller as

$$u_{\mathrm{ILC}} = c_P \sum_{i=1}^{N_{\mathrm{AC}}}\sum_{j=1}^{N_{\mathrm{DC}}} \mathrm{sig}\left[a^{\mathrm{ILC}}_{\mathrm{AC}i}\lambda_i - a^{\mathrm{ILC}}_{\mathrm{DC}j}\lambda_j\right]^{\beta}, \tag{7}$$

where $c_P > 0$ and $\beta \in (0, 1)$ are parameters for regulating the convergence speed. Eq. (7) performs the error between averaging IC measurements between AC and DC MGs. The order of terms in (7) suggests a positive value for a power transferring from the DC to AC MG; u_{ILC} is negative otherwise.

A finite-time algorithm has been added in (7) based on [26], [29] for a faster convergence and small disturbance rejection. Moreover, the PI structure of (6) provide robustness in the face of disturbances due to variation of parameters or not modeled dynamics.

The proposed protocol in (7), (6) gives the following result.

Theorem 1: Consider the control protocol described in (7) *and* (6) *implemented by the ILC of a hybrid MG. Under a balanced graph with a spanning tree in the AC and DC sub-MGs, the IC synchronizes in finite-time* $t_f \leq \frac{V(0)^{1-p}}{M(1-p)}$ $\forall\, M > 0$ *and* $0 < p < 1$.

Proof: It is assumed that $N = N_{\mathrm{AC}} = N_{\mathrm{DC}}$ and $a^{\mathrm{ILC}}_{\mathrm{AC}} = a^{\mathrm{ILC}}_{\mathrm{DC}}$ for the sake of simplicity. This allows

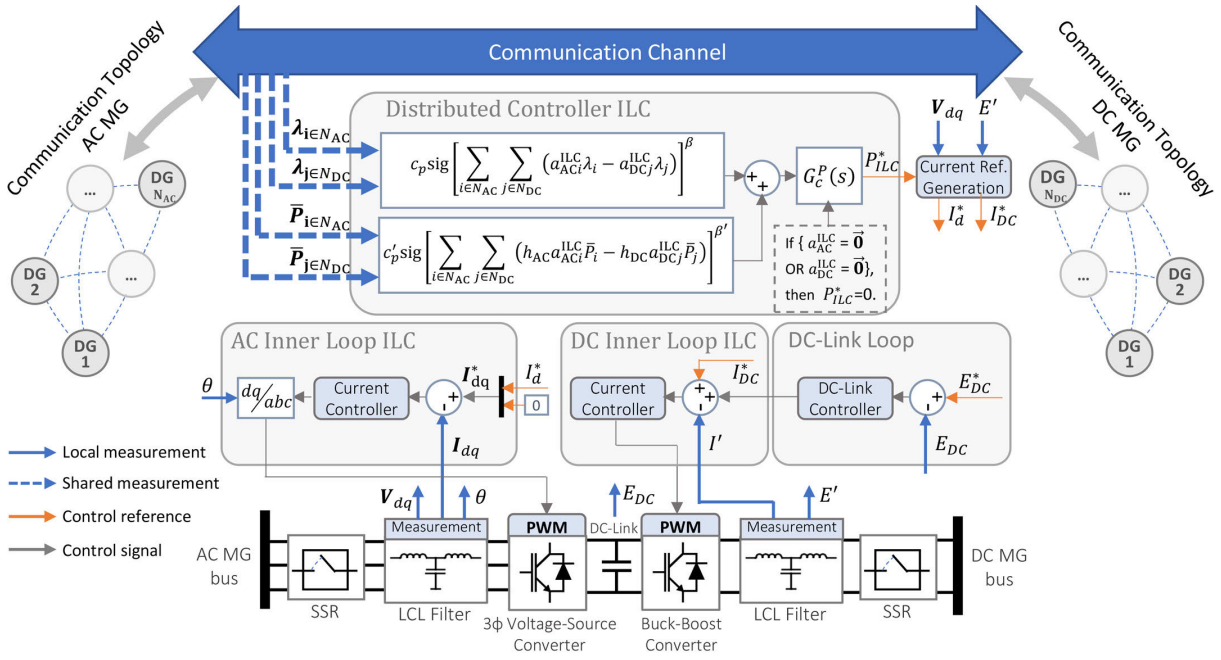

FIGURE 3. Proposed control scheme for the ILC.

the ICs to be paired, and the tracking error to be constructed as $e_i^\lambda = \lambda_i^{\text{AC}} - \lambda_i^{\text{DC}}$. Also, it is defined $\dot{e}_i^\lambda = c_P \sum_{j=1}^N a_{ij} \text{sig}\left[e_j^\lambda - e_i^\lambda\right]^\beta$ with

$$[a_{ij}]_{N\times N} \simeq \begin{bmatrix} 0 & a_{\text{AC1}}^{\text{ILC}} a_{\text{AC2}}^{\text{ILC}} & \dots & a_{\text{AC1}}^{\text{ILC}} a_{\text{ACN}}^{\text{ILC}} \\ a_{\text{AC2}}^{\text{ILC}} a_{\text{AC1}}^{\text{ILC}} & 0 & & a_{\text{AC2}}^{\text{ILC}} a_{\text{ACN}}^{\text{ILC}} \\ \vdots & & \ddots & \vdots \\ a_{\text{ACN}}^{\text{ILC}} a_{\text{AC1}}^{\text{ILC}} & a_{\text{ACN}}^{\text{ILC}} a_{\text{AC2}}^{\text{ILC}} & \dots & 0 \end{bmatrix}. \quad (8)$$

Let $V = \frac{1}{2} e^\lambda (e^\lambda)^T$ be a Lyapunov candidate, with $e^\lambda = (e_1^\lambda, \dots, e_N^\lambda)$, then

$$\dot{V} = (e^\lambda)^T \dot{e}^\lambda = \sum_{i,j=1}^N c_P e_i^\lambda a_{ij} \text{sig}\left[e_j^\lambda - e_i^\lambda\right]^\beta. \quad (9)$$

From (*Lemma 2* [26]), one has

$$\dot{V} \leq -\frac{1}{2}\left(\sum_{i,j=1}^N (c_P a_{ij})^{\frac{2}{1+\beta}} (e_j^\lambda - e_i^\lambda)^2\right)^{\frac{1+\beta}{2}}. \quad (10)$$

By defining $A^\lambda = [(c_P a_{ij})^{(2/(1+\beta))}]$, it results in

$$\dot{V} \leq -\frac{1}{2}\left((e^\lambda)^T L(A^\lambda)\, e^\lambda\right)^{\frac{1+\beta}{2}}. \quad (11)$$

From (*Lemma 3* [26]), one has

$$2(e^\lambda)^T L(A^\lambda)\, e^\lambda \geq 2\,\gamma_2\left(L(A^\lambda)\right)(e^\lambda)^T e^\lambda > 0, \quad (12)$$

with $\gamma_2(L(A^\lambda))$ as the second eigenvalue of $L(A^\lambda)$. Recalling $2\,V = (e^\lambda)^T e^\lambda$ and replacing (12) into (11), it gives

$$\begin{aligned} \dot{V} &\leq -\frac{1}{2}\left(4\gamma_2(L(A^\lambda))V\right)^{\frac{1+\beta}{2}} \\ &\leq -2^\beta \gamma_2(L(A^\lambda))^{\frac{1+\beta}{2}} V^{\frac{1+\beta}{2}} \\ &\leq -MV^p, \end{aligned} \quad (13)$$

where $M = 2^\beta \gamma_2(L(A^\lambda))^{(1+\beta)/2}$ and $p = (1+\beta)/2$ are positive constants as long as $c_P > 0$ and $\beta \in (0,1)$. Therefore, (13) satisfies (*Lemma 1* [26]), i.e. $V(t)$ reaches zero at finite time t_f. ■

C. PARAMETERS FOR THE PROPOSED IC CONTROLLER

Since the IC of each MG is received from several DGs (for reliability purposes), the communication vectors of the ILC need to apportion the information for a generalized compatibility (any number of communicating DGs per MG). Hence, the weights of the communication vector for the ILC respecting the AC MG are designed as

$$a_{\text{AC}\,i}^{\text{ILC}} = \begin{cases} \dfrac{1}{N_{\text{AC}}^{\text{ILC}}}, & \text{if } i\text{-th DG communicates} \\ 0, & \text{otherwise} \end{cases} \quad (14)$$

where $N_{\text{AC}}^{\text{ILC}}$ is the number of active nodes in the AC MG sending information to the ILC. The weights for the communication vector $a_{\text{DC}}^{\text{ILC}}$ can be derived analogically.

The PI controller of power in the ILC is tuned assuming a unit plant, decoupled from the ILC's inner current controller and the subgrids' IC consensus. The design control bandwidth is selected as $\omega_{\text{ILC}} = \min(\omega_{\text{sec}}^{\text{AC}}, \omega_{\text{sec}}^{\text{DC}})$, where $\omega_{\text{sec}}^{\text{AC}}$ and $\omega_{\text{sec}}^{\text{DC}}$ are the secondary control bandwidths applied into the AC and DC MGs, respectively.

IV. DESIGN OF A MULTI-OBJECTIVE DISTRIBUTED CONTROL STRATEGY FOR THE INTERLINKING CONVERTER

Based on the previous formulation, an additional control goal can be incorporated into (7) if the average power of each MG is considered [24]. The idea behind this is to regulate a trade-off between an economic and safety operation. Undoubtedly, imposing power constraints to the subgrids can help to reserve energy in the dispatchable DGs. These reserves are crucial for dealing with local transients [1]. Also, saving in the generated average power of a MG may directly reduce the lines' utilization and increase the useful life of assets. The estimation of a MG average power is feasible to obtain by means of a distributed observer of power performed in every DG [32]. This kind of observer can be construct as follows:

$$\bar{P}_i = P_i + \int_0^t \left(\sum_{j\in\mathcal{N}_i} a_{ij} \operatorname{sig}\left[\bar{P}_j - \bar{P}_i\right]^{\alpha_p} \right) d\tau, \qquad (15)$$

where $\bar{P}_i$ is the average power estimation realized by the i-th DG in a MG, P_i is the measured power of the local DG. The coefficient $0 < \alpha_p < 1$ regulates the convergence rate.

A. DISTRIBUTED MULTI-OBJECTIVE CONTROL FOR ECONOMIC DISPATCH AND POWER REGULATION

The multi-objective control design of the ILC begins by adding a compensation term u_{ILC} into the control input of (6). This new term yields the difference between the average power of AC and DC MGs informed by the DGs. Also, because of the inherent trade-off between IC and average power regulation, a weight is added to regulate the average power balancing. The resulting controller is given by:

$$\begin{aligned} P^*_{\mathrm{ILC}} &= k_p^P(u_{\mathrm{ILC}} + u'_{\mathrm{ILC}}) + k_i^P \int_0^t (u_{\mathrm{ILC}} + u'_{\mathrm{ILC}}) d\tau \\ u'_{\mathrm{ILC}} &= c'_P \sum_{i=1}^{N_{\mathrm{AC}}} \sum_{j=1}^{N_{\mathrm{DC}}} \operatorname{sig}\left[h_{\mathrm{AC}}\, a_{\mathrm{AC}i}^{\mathrm{ILC}} \bar{P}_i - h_{\mathrm{DC}}\, a_{\mathrm{DC}j}^{\mathrm{ILC}} \bar{P}_j \right]^{\beta'}, \end{aligned} \qquad (16)$$

where c'_P is a scaling coefficient, β' is a fractional exponent for convergence, h_{AC} and h_{DC} are weights regulating the trade-off in the control objective, and $\bar{P}_i$ and $\bar{P}_j$ are the average power estimation of the i-th DG in the AC MG and the j-th DG in the DC MG, respectively. For implementation, (16) is simplified by $\beta' = 1$, giving a conventional asymptotic protocol and avoiding unnecessary chattering. The proposed control scheme is resumed in Fig. 3, where $G_c^P(s)$ represents a PI controller transfer function with a logic to clamp the output in case of a complete loss of communications. The use of (16) by the ILC gives rise to the following result

Theorem 2: Consider the control protocol described in (16) *implemented by the ILC of a hybrid MG. Under a balanced graph with a spanning tree in the AC and DC sub-MGs, the IC synchronizes in a proportion given by the average power difference at a finite-time* $t_f \leq \frac{V(0)^{1-p}}{M(1-p)}$ $\forall$ $M > 0$ *and* $0 < p < 1$.

Proof: Based on Theorem 1, the tracking errors are $e_i^\lambda = \lambda_i^{\mathrm{AC}} - \lambda_i^{\mathrm{DC}}$ and $e_i^P = h_{\mathrm{AC}}\bar{P}_i^{\mathrm{AC}} - h_{\mathrm{DC}}\bar{P}_i^{\mathrm{DC}}$. Let $V = V_\lambda + V_P = 1/2\,(e^\lambda(e^\lambda)^T + e^P(e^P)^T)$ be a Lyapunov candidate. For simplicity, it is assumed $\beta = \beta'$; by following the steps of Theorem 1 (*Lemma 2* [26] and *Lemma 3* [26]), one can get

$$\begin{aligned} \dot{V} &\leq -\frac{1}{2}\left(\sum_{i,j=1}^{N} (c_P a_{ij})^{\frac{2}{1+\beta}} (e_j^\lambda - e_i^\lambda)^2 \right)^{\frac{1+\beta}{2}} \\ &\quad - \frac{1}{2}\left(\sum_{i,j=1}^{N} (c'_P a_{ij})^{\frac{2}{1+\beta}} (e_j^P - e_i^P)^2 \right)^{\frac{1+\beta}{2}} \\ \dot{V} &\leq -2^\beta \left(\gamma_1 (L(A^\lambda))^{\frac{1+\beta}{2}} V_\lambda^{\frac{1+\beta}{2}} \right. \\ &\quad \left. + \gamma_2 (L(A^P))^{\frac{1+\beta}{2}} V_P^{\frac{1+\beta}{2}} \right) \\ \dot{V} &\leq -MV^p, \end{aligned} \qquad (17)$$

where $A^P = [(c'_P a_{ij})^{(2/(1+\beta'))}]$, $p = (1+\beta)/2$, $M = 2^\beta \gamma^p$ and $\gamma = \frac{(\gamma_1(L_\lambda))^2 + (\gamma_2(L_P))^2 - \left|(\gamma_1(L_\lambda))^2 - (\gamma_2(L_P))^2\right|}{2\left((\gamma_1(L_\lambda))^2 + (\gamma_2(L_P))^2\right)^{\frac{1}{2}}}$.

Coefficients p and M are positive $\Leftrightarrow \{c_P, c'_P\} \in (0, \infty)$ and $\{\beta, \beta'\} \in (0, 1)$, which completes the proof. ■

B. PARAMETERS FOR THE PROPOSED MULTI-OBJECTIVE CONTROLLER

The parameters of the PI controller are the same of Section III. Regarding the weight used for the trade-off between control goals, values around [0,1] are recommended. Fine-tuning can be conducted through off-line Pareto optimality studies [1], [11]. However, since this control action is only required when power is near the specified boundaries, h coefficients can be calculated online with an adaptive formula depending on the MG saturation. For this purpose, this work proposes an activation function with an exponential shape given by

$$h(\bar{P}_x) = k_h^1\, e^{(k_h^2 \bar{P}_x)}, \qquad (18)$$

where the sub-index x represents either the AC or DC MG. The form of (18) is selected because it gives a smooth and gradual increasing in the average power balance when $\bar{P}_x \rightarrow 1$. The parameters of (18) are selected such that $h(1.0) = 0.9$, i.e. nearly 90% of the ILC capacity is employed for average power balance when a MG is at maximum capacity. This behavior is illustrated in Fig. 4.

V. CASE STUDIES

Performance evaluations of the proposed controllers are made through experimental tests and simulations. The experimental tests were conducted in a laboratory environment with a small hybrid MG testbed in order the validate the controllers in (1) and (16). Subsequently, simulations were yielded to further analyze the behavior of the ILC in face of communication delays and changes in the trade-off policy. The simulation

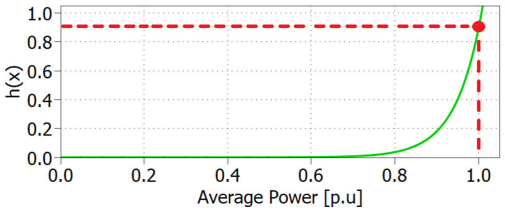

FIGURE 4. Weight function for average power regulation.

environment was necessary to allow the load impacts of different simulations to occur at the same time-step — this permits the waveforms to be overlapped and presented in the same chart for detailed analysis. Also, the simulated MG represents an extended version of the experimental testbed MG, with extra DGs and loads. Three cases are explored, both in the aforementioned experimental and simulated environments. These cases of study are the following:

1) CASE 1. LOAD CHANGING OPERATION

This is a base case for all the tests. The response of the ILC's controller is studied under controlled load impacts, first at the DC MG and then at the AC MG. The impacts' magnitude are described in Table 1. Cases 2 and 3 subdue the hybrid MG to the same load impacts than Case 1.

2) CASE 2. COMMUNICATION DELAYED OPERATION

The ILC's controller is subject to constant time delays in all its communication links. For the experimental tests, it is used a constant delay τ of 400 [ms]. The values of delay τ used for simulations are 125, 250 and 500 [ms]. Also, the DG1 of AC MG loses communication in some point prior to the AC load impacts.

3) CASE 3: MULTI-OBJECTIVE OPERATION

The behavior of the ILC's controller is studied under different values of h_{AC} and h_{DC}. For experimental tests, the adaptive formula (18) is used. For the simulations, values of h_{AC} and h_{DC} equals to 0, 0.2, 0.4, and the adaptive formula (18) are used.

It is worth noting that an stability analysis of a hybrid AC/DC MG that uses distributed controllers, like the proposed ones in this work, is being studied and will be published in a separate work. Details about the simulated and experimental settings are now provided.

A. SIMULATED MG

The simulations are performed in software PLECS. The hybrid MG used for simulations is shown in Fig. 5; it incorporates 5 DGs and 3 loads per MG. The electrical parameters of the system are based on the testbed hybrid MG [33] and are listed in Table 1. Control parameters are shown in Tables 2-3; details about droop and secondary control gains used by the DGs are given in the Appendix.

The economic function parameters in DC MG are 1/2 of the ones shown in Table 2. The power constraints for the converters are the following; $P_i^{\max} = 1$ [kW] $\forall\, i \in \mathcal{N}_{\text{HYB}}$, $Q_i^{\max} = 0.25$ [kVAR] $\forall\, i \in \mathcal{N}_{\text{AC}}$ and $P_{\text{ILC}}^{\max} = 5$ [kW]. The ILC has the communication vectors $a_{\text{AC}}^{\text{ILC}} = (1, 0, 0, 0, 1)$ and $a_{\text{DC}}^{\text{ILC}} = (1, 0, 0, 1, 0)$.

For the tests, a load impact in the DC side is introduced with the connection of Z6. Subsequently, a second and a third load impacts take place on the AC MG; the AC load impacts correspond to the connection and disconnection of Z1.

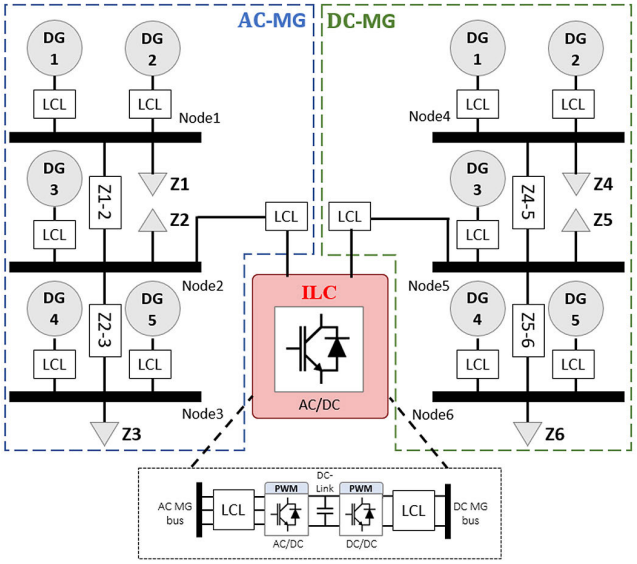

FIGURE 5. Simulated hybrid MG structure. The ILC block represents the AC/DC converter depicted in Fig.3.

TABLE 1. System parameters of hybrid MG.

Parameter	Value	Parameter	Value
Nom. Freq.	50 [Hz]	Line R1-2	1 [mΩ]
Nom. Volt. AC	120 [$V_{1\Phi}$]	Line R2-3	1 [mΩ]
Load Z1	15 [Ω]	Line L1-2	2.50 [mH]
Load Z2	33 [Ω]	Line L2-3	2.50 [mH]
Load Z3	12 [Ω]		
Nom. Volt. DC	100 [V]	Line R4-5	0.17 [Ω]
Load Z4	11 [Ω]	Line R5-6	0.50 [Ω]
Load Z5	8 [Ω]	Line L4-5	2.50 [mH]
Load Z6	16 [Ω]	Line L5-6	2.50 [mH]

TABLE 2. Economic function parameters in AC MG.

Param.	DG1	DG2	DG3	DG4	DG5
a_{ci} [\$/kW^2]	0.264	0.444	0.400	0.500	0.250
b_{ci} [\$/kW]	0.067	0.111	0.100	0.125	0.063
c_{ci} [\$]	51.00	31.00	78.00	42.00	51.00

TABLE 3. Control parameters of the ILC.

Parameter	Value	Parameter	Value
k_p^P	0.25	β	0.70
k_i^P	1.57	β'	1.00
c_P	1000	k_h^1	$1\text{x}10^{-7}$
c_P'	4000	k_h^2	16

B. EXPERIMENTAL SETUP

The testbed MG topology used for experimental validations is a reduced version of the one shown in Fig. 5, with the absence

FIGURE 6. Components of experimental testbed hybrid AC/DC MG [33].

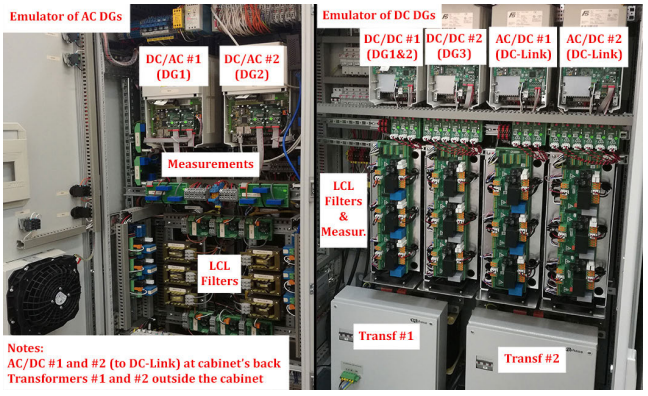

FIGURE 7. Detailed view of equipment and configuration of DG's emulators.

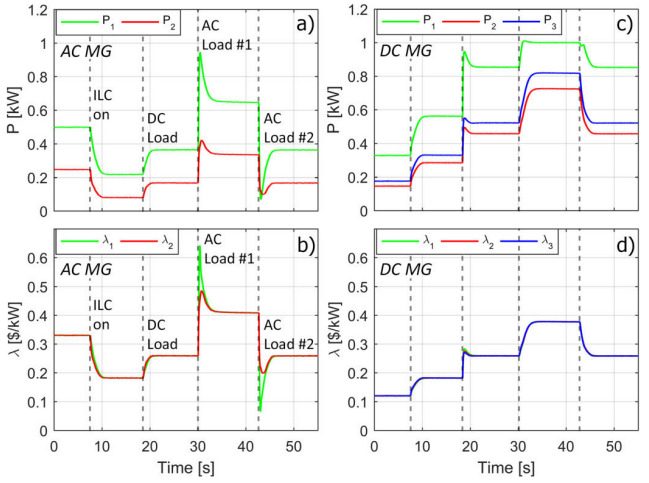

FIGURE 8. MATLAB data logging of the experimental waveforms of hybrid MG under controller in (16) and *h*-coefficient in (18). a) active powers in AC MG, b) ICs in AC MG, c) powers in DC MG, d) ICs in DC MG.

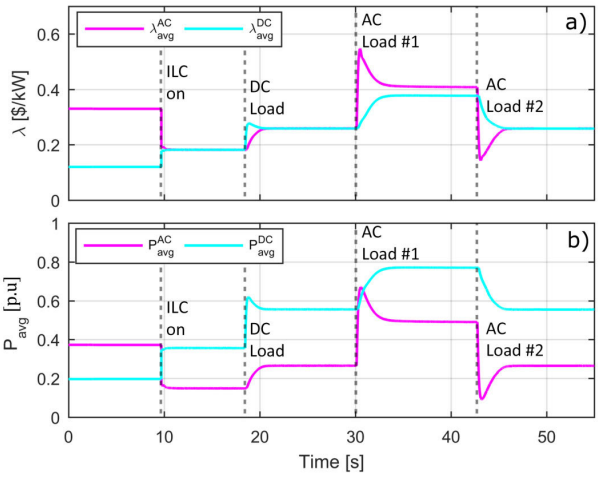

FIGURE 9. MATLAB data logging of the experimental waveforms of the ILC under controller in (16) and *h*-coefficient in (18), a) average calculation of ICs in ILC, b) average calculation of average powers in ILC.

of Z3 and Z5. The generation is composed of DG1 and DG4 (renamed as DG2) in the AC side, and DG1, DG3 (renamed as DG2) and DG4 (renamed as DG3) in the DC side. The DGs are emulated through an industrial modular equipment of the Triphase brand; it consist of multiple 15 [kVA] back-to-back converters with a 16 [kHz] real-time embedded measurement and control system [33]. The experimental AC and DC MG distribution systems are built in separate racks as shown in Fig. 6. Details inside the DG's emulators are shown in Fig. 7.

Control parameters for the DGs and power constraints are the same used by simulations. The control parameters for the ILC are the same than Table 3, excepting $k_i^P = 0.78$ and $\beta = 0.5$. In terms of communication, the ILC has the vectors $a_{\text{AC}}^{\text{ILC}} = (1, 1)$ and $a_{\text{DC}}^{\text{ILC}} = (1, 0, 1)$.

VI. RESULTS AND DISCUSSION

A. EXPERIMENTAL RESULTS

The results under load changes are presented in Fig. 8 and Fig. 9. From Fig. 8, adequate operation under load impacts can be seen in the AC and DC side MGs. At $t = 8$ [s], the ILC controller is activated, showing a smooth transient in both sides; then, at $t = 19$ [s], the first load impact occurs in the DC MG accompanied with another small transient. For both cases, the system quickly stabilizes to seamless find its economic operation point, within a 2 [s] time-span. For the instant $t = 30$ [s], the effect of the load impact that occurred on the AC side can be seen, with a more pronounced transient than in the DC case. Finally, at $t = 43$ [s], a second load impact is seen in the AC MG of equal magnitude but opposite sign to the previous one. Both impact loads recover in about three seconds, roughly doubling the settling-time of the DC side's load impact.

On the IC waveforms in Fig. 9, it can be seen that the ILC quickly equates the ICs, within the described settling times of the previous paragraph. Between $t = 30$ [s] and $t = 43$ [s], it can be seen that the DC MG is near 80% of its capacity, so the

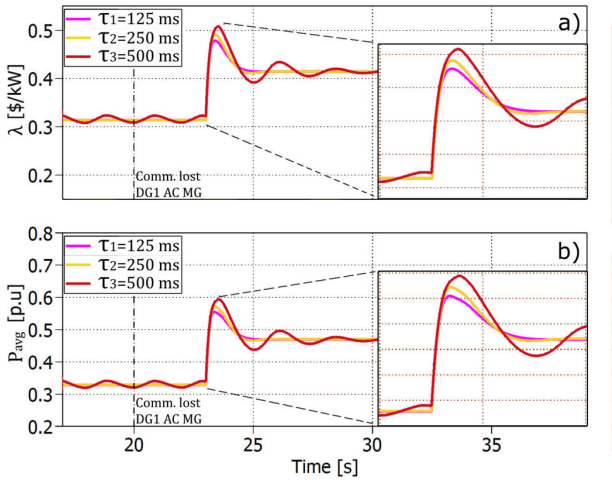

FIGURE 10. Simulation results of the ILC under different time-delays, a) average calculation of IC in AC MG, b) average calculation of average power in AC MG.

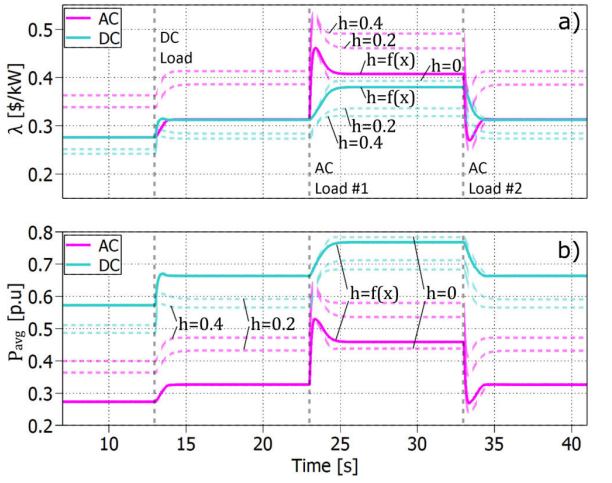

FIGURE 11. Simulation results of the ILC under different *h*-coefficients, a) average calculation of IC in AC and DC MGs, b) average calculation of average power in AC and DC MGs.

IC balancing of the ILC is relaxed. After $t = 43$ [s], the IC balancing recovers its fitness. The results show that the ILC is capable of act near the IC consensus bandwidth of the subgrids secondary control, ensuring an optimal operation of the hybrid MG at almost all times (except during the short transients).

B. SIMULATION RESULTS

1) COMMUNICATION DELAYED OPERATION

Fig. 10 shows how the ILC's settling-time increases as the transport delay do. An oscillatory response can be seen with large delays due to the finite-time protocol; nevertheless, this effect can be neglected by reducing the ILC's control bandwidth or increasing the β exponent — i.e. the finite-time convergence speed can be reduced to avoid system instability. In general, the ILC responds adequately to delays $\tau < \tau_{\max}$, where $\tau_{\max} \approx 785$ [ms] by using (8) and the procedure described in [28].

At $t = 28$ [s] the communication of DG1 in the AC MG is lost, however, it does not affect the controller performance in any form (provided there is another DG in the same MG communicating). Therefore, given the ILC's control bandwidth and the weighting structure used for communication vectors, a resilient behavior is seen, being able to operate under large delays even if it loses some of its communication links.

2) MULTI-OBJECTIVE OPERATION

Fig. 11 presents the results under different h coefficients. It can be seen that the choice of such coefficients gives rise to variations on ICs and average power rating between MGs. The higher the h coefficient, the greater the deviation of ICs is. Also, it is shown that the regulation of ICs is very sensitive to the h weight parameter; hence, this suggests that only small values should be used and when it is strictly necessary. Evidently, using the adaptive formula in (18) gives better results, allowing the operation of one of the MGs to be safeguarded above 80 %, maintaining an appropriate trade-off between the control objectives.

VII. CONCLUSION

This paper demonstrated through experimental tests and simulations the feasibility of a multi-objective control strategy for the ILC in a hybrid AC/DC MG. The proposed ILC's controller relies only on shared measurements of IC and average power to calculate the power reference to be transferred between subgrids. It has been proven that the proposed protocol is resilient against partial communication failures and transport delays. Also, the protocol can ensure a finite-time convergence of control goals, as demonstrated in Theorems 1 and 2. In terms of the design, the weights for the average power balancing showed to be highly sensitive, encouraging caution in its tuning.

Overall, the multi-objective proposal may be applicable in real MG implementations to avoid the operation outside safety limits; in particular, preventing the saturation of one MG while ensuring a fast and decoupled operation. Conversely to decentralized approaches for the ILC, the proposed strategy allows the application of secondary control on the AC and DC subgrids.

Limitations of the proposed method for controlling the ILC are mainly related to communications; The tuning of finite-time parameters in presence of large delays is limited. Also, the complete loss of communications with one subgrid clamps the ILC's output to zero. Future research can be conducted for developing a controller that copes with data and communication losses. Furthermore, using the proposed controllers for enlarged topologies such as meshed hybrid AC/DC MGs with multiple subgrids and multiple ILCs are open research lines to follow.

APPENDIX
CONTROL PARAMETERS OF DGs

Control used for the DGs in AC MG:

$$\omega_i = \omega_i^* - m_i^{\mathrm{AC}} \left(\frac{\omega_c^{\mathrm{AC}}}{s + \omega_c^{\mathrm{AC}}} \right) p_i + \delta\omega_i^1 + \delta\omega_i^2$$

$$\dot{\delta\omega_i^1} = c_\omega(\omega^* - \omega_i) + c_\omega \sum_{j=1}^{N_{\text{AC}}} a_{ij}^{\text{AC}}(\delta\omega_j^1 - \delta\omega_i^1)$$

$$\dot{\delta\omega_i^2} = c_\lambda^{\text{AC}} \sum_{j=1}^{N_{\text{AC}}} a_{ij}^{\text{AC}}(\lambda_j - \lambda_i)$$

$$V_i = V_i^* - n_i^{\text{AC}} \left(\frac{\omega_c^{\text{AC}}}{s + \omega_c^{\text{AC}}} \right) q_i + \delta V_i$$

$$\dot{\delta V_i} = c_E^{\text{AC}}(\bar{V} - V_i) + c_Q k_i^Q \sum_{j=1}^{N_{\text{AC}}} a_{ij}^{\text{AC}} \left(\frac{Q_j}{Q_j^{\max}} - \frac{Q_i}{Q_i^{\max}} \right) + c_Q k_p^Q \sum_{j=1}^{N_{\text{AC}}} a_{ij}^{\text{AC}} \left(\frac{\dot{Q}_j}{Q_j^{\max}} - \frac{\dot{Q}_i}{Q_i^{\max}} \right)$$

with $\omega_c^{\text{AC}} = 6.28$, $m^{\text{AC}} = 2.8\text{x}10^{-3}$, $c_\omega = 0.15$, $c_\lambda^{\text{AC}} = 0.14$, $n^{\text{AC}} = 1.4\text{x}10^{-2}$, $c_E^{\text{AC}} = 47.12$, $c_Q = 12$, $k_p^Q = 0.05$, $k_i^Q = 1.57$.

Control used for the DGs in DC MG:

$$E_i = E_i^* - m_i^{\text{DC}} \left(\frac{\omega_c^{\text{DC}}}{s + \omega_c^{\text{DC}}} \right) p_i + \delta E_i$$

$$\dot{\delta E_i} = c_E^{\text{DC}}(\bar{E} - E_i) + c_\lambda^{\text{DC}} k_i^\lambda \sum_{j=1}^{N_{\text{DC}}} a_{ij}^{\text{DC}} (\lambda_j - \lambda_i) + c_\lambda^{\text{DC}} k_p^\lambda \sum_{j=1}^{N_{\text{DC}}} a_{ij}^{\text{DC}} (\dot{\lambda}_j - \dot{\lambda}_i)$$

with $\omega_c^{\text{DC}} = 18.85$, $m^{\text{DC}} = 3.0\text{x}10^{-3}$, $c_E^{\text{DC}} = 4.71$ $c_\lambda^{\text{DC}} = 400$, $k_p^\lambda = 0.28$, $k_i^\lambda = 0.54$.

REFERENCES

[1] D. E. Olivares, A. Mehrizi-Sani, A. H. Etemadi, C. A. Cañizares, R. Iravani, M. Kazerani, and A. H. Hajimiragha, "Trends in microgrid control," *IEEE Trans. Smart Grid*, vol. 5, no. 4, pp. 1905–1919, Jul. 2014.

[2] X. Liu, P. Wang, and P. C. Loh, "A hybrid AC/DC microgrid and its coordination control," *IEEE Trans. Smart Grid*, vol. 2, no. 2, pp. 278–286, Jun. 2011.

[3] S. K. Sahoo, "Control techniques in AC, DC, and hybrid AC-DC microgrid: A review," *IEEE J. Emerg. Sel. Topics Power Electron.*, vol. 6, no. 2, pp. 738–759, Jun. 2018.

[4] X. Lu, J. M. Guerrero, K. Sun, J. C. Vasquez, R. Teodorescu, and L. Huang, "Hierarchical control of parallel AC-DC converter interfaces for hybrid microgrids," *IEEE Trans. Smart Grid*, vol. 5, no. 2, pp. 683–692, Mar. 2014.

[5] Y. Xia, Y. Peng, P. Yang, M. Yu, and W. Wei, "Distributed coordination control for multiple bidirectional power converters in a hybrid AC/DC microgrid," *IEEE Trans. Power Electron.*, vol. 32, no. 6, pp. 4949–4959, Jun. 2017.

[6] E. Espina, R. Cardenas-Dobson, J. W. Simpson-Porco, D. Saez, and M. Kazerani, "A consensus-based secondary control strategy for hybrid AC/DC microgrids with experimental validation," *IEEE Trans. Power Electron.*, vol. 36, no. 5, pp. 5971–5984, May 2021.

[7] J. M. Guerrero, J. C. Vasquez, J. Matas, L. García de Vicuna, and M. Castilla, "Hierarchical control of droop-controlled AC and DC microgrids—A general approach toward standardization," *IEEE Trans. Ind. Electron.*, vol. 58, no. 1, pp. 158–172, Jan. 2011.

[8] E. Espina, J. Llanos, C. Burgos-Mellado, R. Cardenas-Dobson, M. Martinez-Gomez, and D. Saez, "Distributed control strategies for microgrids: An overview," *IEEE Access*, vol. 8, pp. 193412–193448, Oct. 2020.

[9] G. Chen, F. L. Lewis, E. N. Feng, and Y. Song, "Distributed optimal active power control of multiple generation systems," *IEEE Trans. Ind. Electron.*, vol. 62, no. 11, pp. 7079–7090, Nov. 2015.

[10] J. Llanos, D. E. Olivares, J. W. Simpson-Porco, M. Kazerani, and D. Saez, "A novel distributed control strategy for optimal dispatch of isolated microgrids considering congestion," *IEEE Trans. Smart Grid*, vol. 10, no. 6, pp. 6595–6606, Nov. 2019.

[11] V. V. S. N. Murty and A. Kumar, "Multi-objective energy management in microgrids with hybrid energy sources and battery energy storage systems," *Protection Control Mod. Power Syst.*, vol. 5, no. 1, pp. 1–20, Jan. 2020.

[12] P. Yang, M. Yu, Q. Wu, P. Wang, Y. Xia, and W. Wei, "Decentralized economic operation control for hybrid AC/DC microgrid," *IEEE Trans. Sustain. Energy*, vol. 11, no. 3, pp. 1898–1910, Jul. 2020.

[13] C. Chen, S. Duan, B. Liu, and G. Hu, "Smart energy management system for optimal microgrid economic operation," *IET Renew. Power Generat.*, vol. 5, no. 3, pp. 258–267, May 2011.

[14] A. A. A. Radwan and Y. A.-R. I. Mohamed, "Networked control and power management of AC/DC hybrid microgrids," *IEEE Sys. J.*, vol. 11, no. 3, pp. 1662–1673, Sep. 2017.

[15] P. C. Loh, D. Li, Y. K. Chai, and F. Blaabjerg, "Autonomous control of interlinking converter with energy storage in hybrid AC–DC microgrid," *IEEE Trans. Ind. Appl.*, vol. 49, no. 3, pp. 1374–1382, May/Jun. 2013.

[16] N. Eghtedarpour and E. Farjah, "Power control and management in a hybrid AC/DC microgrid," *IEEE Trans. Smart Grid*, vol. 5, no. 3, pp. 1494–1505, May 2014.

[17] Q. Xu, J. Xiao, P. Wang, and C. Wen, "A decentralized control strategy for economic operation of autonomous AC, DC, and hybrid AC/DC microgrids," *IEEE Trans. Energy Convers.*, vol. 32, no. 4, pp. 1345–1355, Dec. 2017.

[18] C. Jin, C. Dong, J. Wang, and P. Wang, "Uniform control scheme for the interlinking converter enhancing the economy and resilience of hybrid AC/DC microgrids," in *Proc. IEEE Innov. Smart Grid Technol.-Asia (ISGT Asia)*, May 2018, pp. 862–866.

[19] Q. Zhou, M. Shahidehpour, Z. Li, and X. Xu, "Two-layer control scheme for maintaining the frequency and the optimal economic operation of hybrid AC/DC microgrids," *IEEE Trans. Power Syst.*, vol. 34, no. 1, pp. 64–75, Jan. 2019.

[20] J. Zhou, H. Zhang, Q. Sun, D. Ma, and B. Huang, "Event-based distributed active power sharing control for interconnected AC and DC microgrids," *IEEE Trans. Smart Grid*, vol. 9, no. 6, pp. 6815–6828, Nov. 2018.

[21] H.-J. Yoo, T.-T. Nguyen, and H.-M. Kim, "Consensus-based distributed coordination control of hybrid AC/DC microgrids," *IEEE Trans. Sustain. Energy*, vol. 11, no. 2, pp. 629–639, Apr. 2019.

[22] P. Lin, C. Jin, J. Xiao, X. Li, D. Shi, Y. Tang, and P. Wang, "A distributed control architecture for global system economic operation in autonomous hybrid AC/DC microgrids," *IEEE Trans. Smart Grid*, vol. 10, no. 3, pp. 2603–2617, May 2019.

[23] W. Feng, J. Yang, Z. Liu, H. Wang, M. Su, and X. Zhang, "A unified distributed control scheme on cost optimization for hybrid AC/DC microgrid," in *Proc. IEEE 4th Southern Power Electron. Conf. (SPEC)*, Dec. 2018, pp. 1–6.

[24] M. M. Gomez, R. C. Dobson, A. N. Fonseca, and E. R. Luengo, "A multi-objective distributed finite-time optimal dispatch of hybrid microgrids," in *Proc. 46th Annu. Conf. IEEE Ind. Electron. Soc. (IECON)*, Oct. 2020, pp. 3755–3760.

[25] F. Guo, C. Wen, J. Mao, and Y. D. Song, "Distributed secondary voltage and frequency restoration control of droop-controlled inverter-based microgrids," *IEEE Trans. Ind. Electron.*, vol. 62, no. 7, pp. 4355–4364, Jul. 2015.

[26] S. Zuo, A. Davoudi, Y. Song, and F. L. Lewis, "Distributed finite-time voltage and frequency restoration in islanded AC microgrids," *IEEE Trans. Ind. Electron.*, vol. 63, no. 10, pp. 5988–5997, Oct. 2016.

[27] A. Bidram, A. Davoudi, and F. L. Lewis, *Cooperative Synchronization in Distributed Microgrid Control: Advances in Industrial Control*. Cham, Switzerland: Springer, 2017.

[28] R. Olfati-Saber and R. M. Murray, "Consensus problems in networks of agents with switching topology and time-delays," *IEEE Trans. Autom. Control*, vol. 49, no. 9, pp. 1520–1533, Sep. 2004.

[29] L. Wang and F. Xiao, "Finite-time consensus problems for networks of dynamic agents," *IEEE Trans. Autom. Control*, vol. 55, no. 4, pp. 950–955, Apr. 2010.

[30] S. P. Bhat and D. S. Bernstein, "Finite-time stability of continuous autonomous systems," *SIAM J. Control Optim.*, vol. 38, no. 3, pp. 751–766, Jan. 2000.

[31] J. Cortés, "Finite-time convergent gradient flows with applications to network consensus," *Automatica*, vol. 42, no. 11, pp. 1993–2000, 2006.

[32] Q. Shafiee, V. Nasirian, J. C. Vasquez, J. M. Guerrero, and A. Davoudi, "A multi-functional fully distributed control framework for AC microgrids," *IEEE Trans. Smart Grid*, vol. 9, no. 4, pp. 3247–3258, Jul. 2018.
[33] E. Espina, C. Burgos-Mellado, J. Gómez, J. Llanos, E. Rute, A. Navas, M. Martinez-Gomez, R. Cardenas, and D. Saez, "Experimental hybrid AC/DC-microgrid prototype for laboratory research," in *Proc. 22nd Eur. Conf. Power Electron. Appl. (EPE ECCE Europe)*, Sep. 2020, pp. 1–9.

MANUEL MARTINEZ-GOMEZ (Graduate Student Member, IEEE) was born in Punta Arenas, Chile. He received the B.Sc. degree in electrical engineering from the University of Magallanes, Punta Arenas, in 2015. He is currently pursuing the dual Ph.D. degree in electrical engineering with the University of Chile, Chile, and the University of Nottingham, U.K. From 2014 to 2017, he was a part-time Lecturer with the University of Magallanes. His research interests include agent control, cooperative control of microgrids, finite-time control, and power electronics applications.

ALEX NAVAS (Graduate Student Member, IEEE) was born in Latacunga, Ecuador. He received the B.Sc. degree in electronic engineering from the Army Polytechnic School—ESPE, Ecuador, in 2015. He is currently pursuing the dual Ph.D. degree in electrical engineering with the University of Chile, Chile, and the University of Nottingham, U.K. His research interests include the control and management of microgrids, model predictive control applied to microgrids, and renewable energies.

MARCOS E. ORCHARD (Member, IEEE) received the M.S. and Ph.D. degrees in electrical and computer engineering from Georgia Institute of Technology, Atlanta, GA, USA, in 2005 and 2007, respectively. He is currently a Professor with the Department of Electrical Engineering, Universidad de Chile, Santiago, Chile, where he is also an Associate Researcher with the Advanced Center for Electrical and Electronic Engineering (UTFSM). He has authored or coauthored more than 100 articles. His current research interests include failure prognosis, electromobility, mining industry, and finance. He is a fellow of the Prognostic and Health Management Society (PHMS).

SERHIY BOZHKO (Senior Member, IEEE) received the M.Sc. and Ph.D. degrees in electromechanical systems from the National Technical University of Ukraine, Kyiv, Ukraine, in 1987 and 1994, respectively. Since 2000, he has been with the Power Electronics, Machines and Control Research Group, University of Nottingham, Nottingham, U.K., where he is currently a Professor of aircraft electric power systems and the Director of the Institute for Aerospace Technology. His research interests include aircraft electric power system areas, including power generation, distribution and conversion, power quality, control and stability issues, power management and optimization, and advanced modeling and simulation methods. He leads several EU- and industry-funded projects in these areas.

CLAUDIO BURGOS-MELLADO (Member, IEEE) was born in Cunco, Chile. He received the B.Sc. and M.Sc. degrees in electrical engineering from the University of Chile, Santiago, Chile, in 2012 and 2013, respectively, and the dual Ph.D. degree in electrical and electronic engineering from the University of Nottingham, U.K., and in electrical engineering from the University of Chile, in 2019. From 2019 to 2021, he was a Research Fellow with the Power Electronics, Machines and Control Group (PEMC Group), University of Nottingham, U.K. He is currently an Assistant Professor with the Institute of Engineering Sciences, Universidad de O'Higgins, Rancagua, Chile. His current research interests include battery energy storage systems, electrical vehicle technologies, power electronics, microgrids, power quality issues, and modular multilevel converters.

ROBERTO CÁRDENAS (Senior Member, IEEE) was born in Punta Arenas, Chile. He received the B.Sc. degree from the University of Magallanes, Chile, in 1988, and the M.Sc. and Ph.D. degrees from the University of Nottingham, U.K., in 1992 and 1996, respectively. From 1989 to 1991 and from 1996 to 2008, he was a Lecturer with the University of Magallanes. From 1991 to 1996, he was with the Power Electronics Machines and Control Group (PEMC Group), University of Nottingham. From 2009 to 2011, he was with the Electrical Engineering Department, University of Santiago. He is currently a Full Professor of power electronics and drives with the Electrical Engineering Department, University of Chile, Chile. His research interests include control of electrical machines, variable speed drives, and renewable energy systems. He received the IEEE–TIE Best Paper Award from the IEEE TRANSACTIONS ON INDUSTRIAL ELECTRONICS, in 2005 and 2019. He is an Associate Editor for the IEEE TRANSACTIONS ON INDUSTRIAL ELECTRONICS.